International Journal of Biological Macromolecules 145 (2020) 100–107

Contents lists available at ScienceDirect

International Journal of Biological Macromolecules

journal homepage: http://www.elsevier.com/locate/ijbiomac

Porous rice starch produced by combined ultrasound-assisted ice recrystallization and enzymatic hydrolysis

Thewika Keeratiburana [a,b], Aleksander Riise Hansen [b], Siriwat Soontaranon [c], Sunanta Tongta [a,*], Andreas Blennow [b,*]

[a] School of Food Technology, Institute of Agricultural Technology, Suranaree University of Technology, 30000, Thailand
[b] Department of Plant and Environmental Sciences, Faculty of Science, University of Copenhagen, Frederiksberg C DK-1871, Denmark
[c] Synchrotron Light Research Institute (Public Organization), Muang, Nakhon Ratchasima 30000, Thailand

ARTICLE INFO

Article history:
Received 13 September 2019
Received in revised form 22 November 2019
Accepted 16 December 2019
Available online 18 December 2019

Keywords:
Porous starch
Physical modification
Enzymatic modification

ABSTRACT

The effects of multicycle ultrasound-assisted ice recrystallization (US+IR) combined with amyloglucosidase (AMG) or maltogenic α-amylase (MA) catalyzed hydrolysis on structure were investigated. Scanning electron microscopy (SEM) showed that the US+IR produced shallow indentations and grooves on the exterior of granules while the combination US+IR and enzyme hydrolysis created additional pores on starch granules. MA displayed a higher number of pores than AMG. The highest values of specific surface area (S_{BET}) and the total pore volume were obtained for US+IR→MA (1.96 $m^2\ g^{-1}$ and 7.26 × 10^{-3} $cm^3\ g^{-1}$, respectively). The US+IR treatment significantly decreased the relative crystallinity, amylose content and swelling capacity. Those parameters were further efficiently decreased following enzymatic hydrolysis. The combined treatments generated products with higher initial gelatinization temperature (Ti) compared to the corresponding controls. The US+IR increased the digestion rate constant (k-value) compared to native starch. However, the combined treatment, US+IR→AMG, significantly decreased the k-value from 2.97 × 10^{-3} to 2.50 × 10^{-3} min^{-1} compared to its control.

Our study demonstrates that US+IR treatment in combination with enzyme hydrolysis is a useful method to produce specifically functionalized porous rice starch that can be used as e.g. absorbents and for further chemical modifications.

1. Introduction

Rice starch is widely used in food and non-food application. The demand is increasing and important characteristics include hypoallergenicity, bland taste, white colour and small granules [1]. However, the use of native starch is limited due to its compact granules, which is less accessibility of chemicals and enzymes, thereby, impeding its use in some applications. Recently, porous starch has attained increasing interest specifically due to the large specific surface areas of this product that can be used as a carrier or absorbent [2,3]. A number of methods have been developed to produce porous starch mainly including physical, chemical and enzymatic protocols. However, especially chemical method can be associated with environmental pollution and increasing consumer concerns. Physical and enzymatic methods are considered to be environmentally friendly as it reduces usage of chemicals and waste.

Freezing-thawing (F/T) of granular starch is a clean and feasible way to functionalize starch by generating higher surface area. [4–6]. F/T combined with enzyme modification further extends this functionality [7]. The F/T principle is based on an initial crystallization of bulk and structured water during the freezing process resulting in physical stress in the granular matrix inducing pore and crack formation [8]. The efficiency of this process is facilitated by using slow freezing rates and multiple F/T cycles [4–6]. Ice recrystallization (IR) is a molecular reorganization process that it characterized by increased size of the ice crystals. This process is the major cause for physical degradation of e.g. starch using F/T. Typically, larger ice crystals are created as a result of temperature fluctuations. A typical F/T protocol involves freezing and thawing of starch granules in water in 20–24 h F/T cycles which is a slow process and ice recrystallization can potentially speed up the process. Additionally, ultrasonic treatment (US) is a physical method attending attraction due to its capability to reorganize starch chains and create pinholes on starch granular surface. In starch-water systems, ultrasound-treatment creates intensive shear force, high temperature, and free radicals which can break the chains of starch thereby changing, and often improving, the properties of starch [9,10].

Enzyme-assisted protocols is gaining in popularity due to the high substrate selectivity, product specificity, mild reaction conditions,

* Corresponding authors.
E-mail addresses: s-tongta@g.sut.ac.th (S. Tongta), abl@plen.ku.dk (A. Blennow).

https://doi.org/10.1016/j.ijbiomac.2019.12.144
0141-8130/

reduced by-products and high safety [11–13]. For porous starch, the most common enzymes are α-amylase and amylogucosidase used separate and in combination [14–17]. However, granular rigidity prevents efficient catalysis using enzymes. Thus, high enzyme dosage is required to sustain reasonable reaction rates, resulting in high-costs [18]. For the purpose to increase reaction rates by increasing the specific surface area of starch, ultrasound treatment have been employed [18–20]. However, the synergy of ice recrystallization and ultrasonic effects might not be sufficient to modify the highly dense and complex starch structure. In this present study, amyloglucosidase (AMG) and maltogenic α-amylase (MA) was used to modify porous rice starch after using physical modifications as a pretreatment. AMG is an *exo*-acting enzyme that hydrolyzes both α,1-4 and α,1-6 linkages from the non-reducing ends of starch chain releasing glucose. On the other hand, MA is versatile enzyme that mainly has exo-action, cleaving α,1-4 glucosidic linkage, generating maltose but also exhibits *endo*-action within the starch chain [11,21]. In addition, MA also has a minor transglycosylation activity forming linkages such as α,1-3 and α,1-6 linkages producing branched oligosaccharides from gelatinized starch [22,23].

This study particularly introduces IR and US to prepare granular rice starch for further enzyme treatment producing highly porous rice starch. To demonstrate the potential of this approach, the morphological, structural, physicochemical and digestibility to amylolytic enzymes were investigated. The results reveal important fundamental mechanisms of combined physical and enzymatic granular starch modification.

2. Materials and methods

2.1. Materials

Rice starch was a gift from General Food Products Co., Ltd. (Nakhon Ratchasima, Thailand). Amyloglucosidase (EC 3.2.1.3, specific activity 260 U mL^{-1}) from *Aspergillus niger* was purchased from Sigma-Aldrich (Steinheim, Germany). Maltogenic α-amylase (EC 3.2.1.133, Maltogenase® L) was kindly provided by Novozymes (Bagsvaerd, Denmark). Porcine pancreatic α-amylase (PPA, EC 3.2.1.1, specific activity 12 U mg^{-1}) and PGO (peroxidase and glucose oxidase) enzyme kit were purchased from Sigma-Aldrich (Missouri, USA).

2.2. Preparation of porous starch

2.2.1. Ultrasound-assisted ice recrystallization (US+IR treatment)

Rice starch (10 g, dry basis) samples were dispersed with 20 mL of distilled water for 3 h in an aluminum box at room temperature. Boxes with starch were stored in a temperature range of 0 to −5 °C to induce ice recrystallization for 6 h followed by thawing in an ultrasonic bath (Bandelin Sonorex Digitec, Berlin, Germany) at frequency of 20 kHz, power 170 W at temperature range of 25–35 °C for 1 h to perform 1 cycle of US+IR. The procedure was repeated in 7 cycles. The starch samples were filtered and dried at 50 °C for 12 h. The dried starch samples were gently ground as powder, passed through a 100-mesh sieve and stored in a desiccator until analysis.

2.2.2. US+IR followed by enzymatic hydrolysis

Starch samples prepared by US+IR (10 g, dry basis) were suspended in 20 mL of 20 mM Na acetate buffer at pH 4.5 (AMG treatment) or 20 mM Na maleate and 5 mM $CaCl_2$ buffer at pH 5.5 (MA treatment). The starch suspensions were pre-heated in water bath at 60 °C for 0.5 h and 100 U g^{-1} starch of AMG or MA solutions were added. The samples were incubated at 60 °C for 12 h in a shaking water bath (180 rpm). The suspensions were centrifuged at 4000*g* and 4 °C for 5 min followed by 3 times washing with 40 mL of MilliQ water. The sediments were pre-dried at 60 °C for 20 min before complete drying at 130 °C for 2 h. The dried starch samples were ground and sieves as described above. Control samples were prepared using the same procedures without enzyme.

2.3. Scanning electron microscopy (SEM)

Granular morphology was investigated using Field Emission Scanning Electron Microscope (FE-SEM, Carl Zeiss, Oberkochen, Germany). Starch samples (1%) were dispersed in absolute ethanol. One drop of each sample was placed on a coverslip and dried at 50 °C for 3 h. A thin layer of each sample was stuck on aluminum stubs with conductive carbon tape and sputter-coated with gold-palladium. The samples were examined at an accelerating voltage of 3.0 kV.

2.4. Specific surface area and total pore volume using nitrogen sorption isotherms through Brumauer-Emmett-Teller (BET) protocol

Prior to measurement, starch samples were dried at 100 °C for 6 h and kept in a desiccator. Dried starch (200 mg) was packed in the sample tube and then degassed at 125 °C for 24 h. The sample tube was placed in BET instrument with purging nitrogen gas and immersed in liquid nitrogen (−196 °C). The measurement was carried out by dispensing a specific portion of the nitrogen gas (2 L) and measuring the relative pressure p/po. The pressure change was recorded by BELSORP-mini II (MicrotracBel Corp., Osaka, Japan). Specific surface area and total pore volume were calculated by BET method [24].

2.5. Relative crystallinity

The crystallinity of starch samples was quantified by wide-angle X-ray scattering (WAXS) as described by Boonna and Tongta [25]. The WAXS data were collected in the 2θ range of 8 to 30°. The relative crystallinity was calculated by the ratio of the relative area of crystalline peaks to the total area using a program called SAXSIT (Small Angle X-ray Scattering Image Tool) developed in-house (BL1.3W: SAXS, Synchrotron Light Research Institute, Nakhon Ratchasima, Thailand) as follows:

$$\text{Relative crystallinity } (\%) = \frac{\text{Area of crystalline peaks}}{\text{Total area of crystalline and amorphous peaks}} \times 100$$

2.6. Determination of amylose content

The apparent amylose content was determined as described by Wickramasinghe, Blennow and Noda [26].

2.7. Molecular weight fraction analysis by size-exclusion chromatography with triple detection array (SEC-TDA)

Firstly, starch samples were prepared in form of non-granular starch as described by Klucinec and Thompson [27]. Non-granular starch (5 mg) was dissolved in 25 μL of 2 M KOH at 4 °C for 24 h. The non-granular starch solution was re-dissolved in 975 μL Milli-Q water and shaken in a Thermomixer (Eppendorf, Germany) at 80 °C for 5 h at 1200 rpm. Then the sample was diluted to 1 mg mL^{-1}. The molecular weight fractions were determined by size exclusion chromatography (SEC) using a Viscotek System (Malvern, UK) equipped with a GS-520HQ column (Shodex) attached to a TDA302 module (Triple detector array) as described by Sorndech et al. [28]. Multidetector homopolymer calibration of the RI, scattering and viscosimetere detectors was made using pullulan (Mw 48,800 Da, dn/dc 0.131, polydispersion 1.07, Showa Denko) as a standard. The flow rate was set at 0.5 mL min^{-1} 10 mM ammonium formate containing 0.02% sodium azide as eluent. The data processing was performed using the OmniSec Software 4.7 (Malvern Instrument, Ltd.).

2.8. Swelling capacity and solubility of starch

The swelling capacity (SC) and solubility (S) were determined on the basis of the method described by Rosell, Yokoyama and Shoemaker [29] with a slight modification. Briefly, 100 mg db of the starch was weighed in centrifuge tubes followed by addition of 10 mL of MilliQ water and heating at 60 °C for 30 min under continuous stirring. After cooling to room temperature, the tubes were centrifuged at 4000*g* for 15 min. The supernatant was collected and the precipitate weighed. The supernatants were transferred to Petri dishes then dried at 110 °C overnight to constant weight. The swelling capacity and solubility were calculated as follows:

$$\text{SC (g/g)} = \text{sediment weight}/[\text{weight of dried starch} \times (1-\text{S}/100)]$$

$$\text{S (\%)} = (\text{dried supernatant weight}/\text{weight of dried starch}) \times 100$$

2.9. Pasting properties

The pasting properties were determined using a Rapid Visco Analyser (RVA) (Newport Scientific, Warriewood, Australia). Starch (2.5 g, 14% moisture content) was added to 25 mL of MilliQ water in the aluminum RVA canister. RVA settings were performed by heating from 50 to 95 °C in 282 s, holding at 95 °C for 150 s and cooling to 50 °C. The initial mixing speed was 960 rpm for 10 s and then 160 rpm paddle speed was followed. Pasting parameters were recorded using Thermocline software (Perten Instruments, Hägersten, Sweden) for Windows.

2.10. Thermal properties

The thermal properties of starch sample were analyzed using differential scanning calorimeter DSC1 instrument (Mettler Toledo, Switzerland). The starch sample (10 mg, db) was mixed with MilliQ water (1:3, w/v) in the stainless-steel pan. The sample pan was hermetically sealed and equilibrated at room temperature for 24 h before analysis. An empty sealed pan was used as a reference. The heating profile was from 25 to 130 °C at a rate of 5 °C min^{-1}. Initial temperature (Ti) defined as the temperature of the sample start to gelatinize, onset temperature (To), peak temperature (Tp), conclusion temperature (Tc), gelatinization temperature range (Tc-Ti) and gelatinization enthalpy (ΔH) were calculated by STAR^e software version 10.0 (Mettler Toledo, Switzerland).

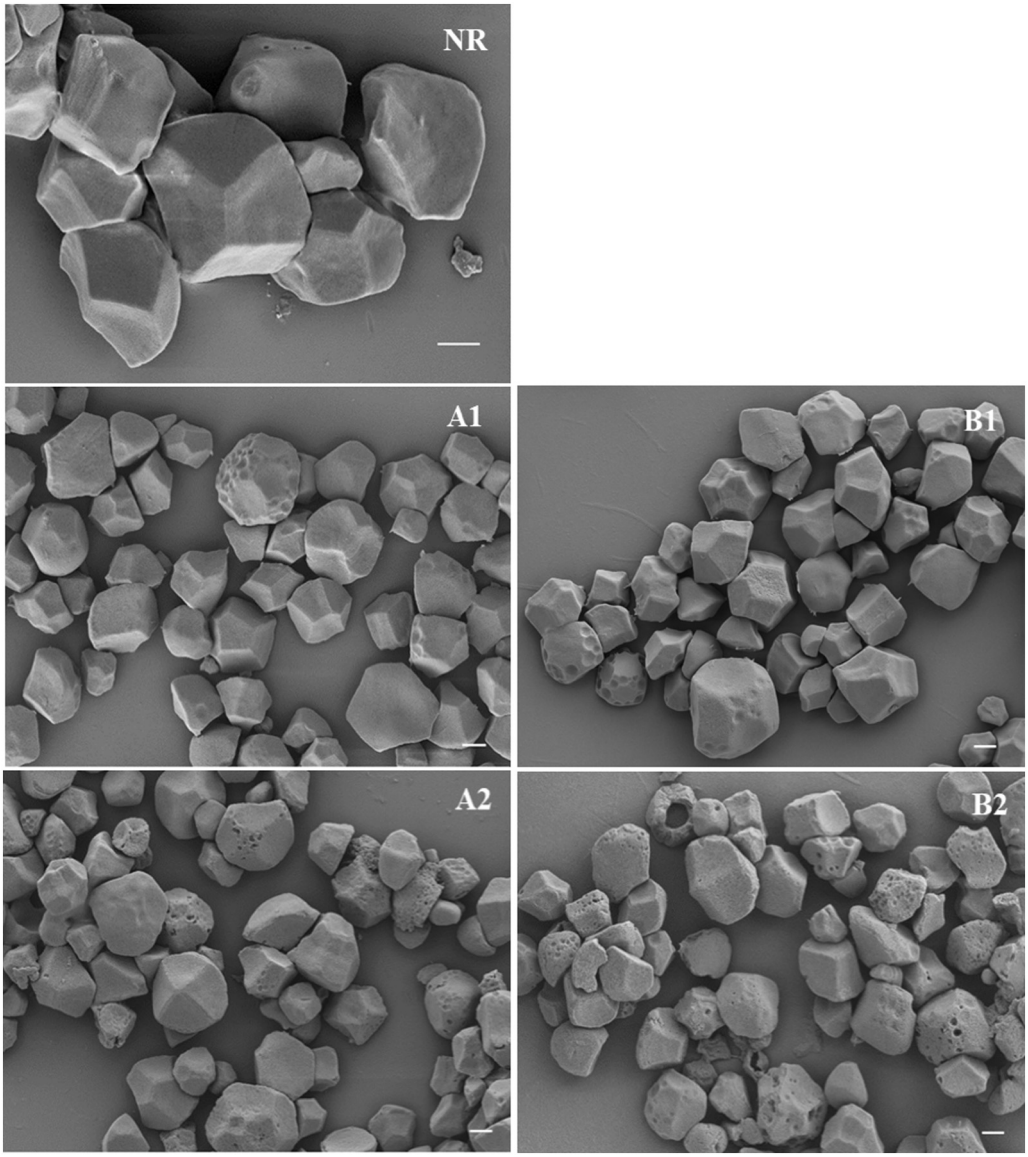

Fig. 1. SEM micrographs for native rice starch (NR), US+IR treated starch (1) and the combination with AMG and MA (2, A; AMG and B; MA). Scale bar = 2 μm.

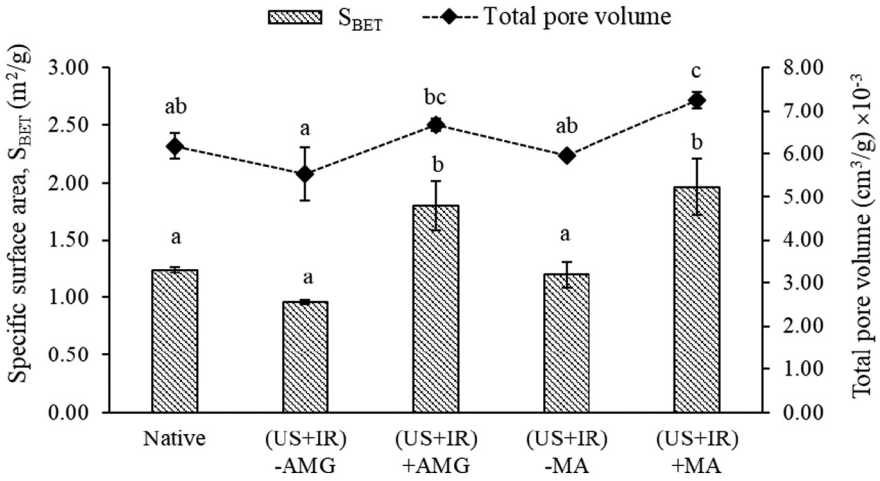

Fig. 2. Specific surface area and total pore volume of starch samples. Different letters represent that samples are statistically different ($p < 0.05$).

2.11. The rate of digestion

The rate of digestion was measured by a modified Englyst method [30]. Free sugars were removed by suspending the starch sample (5 mg) in 200 μL of ethanol (80%, w/w), incubation at 85 °C for 5 min in a shaking water bath (180 rpm) and centrifugation at 15,000*g* for 5 min. The starch was collected and incubated in 250 μL of 0.2 M phosphate buffer (pH 6) with 30 U of PPA and 1 U of AMG at 37 °C for 0, 10, 20, 30, 45, 60, 120, 180, 240, 360 and 1440 min in a shaking incubator (120 rpm). Hydrolysis was terminated by adding 250 μL of ethanol (96%, w/w) and sample was centrifuged at 15,000*g* for 5 min at 4 °C. The starch digestion rate was measured as the percentage of glucose released over the time course using the PGO enzyme assay (Sigma-Aldrich, Missouri, USA). The experimental data were fitted to a first order kinetic model, $C = 1\text{-}e^{kt}$, where t is the digestion time (min), C is the concentration of product at time t, and k is the digestion rate constant (min^{-1}). The experiments were carried out in triplicate.

2.12. Statistical analysis

The data were analyzed for analysis of variance (ANOVA), followed by Duncan's multiple-range test using the SPSS 22.0 statistical software program (SPSS, Incorporated, Chicago). A level of 0.05 was considered statistically significant.

3. Results and discussion

A 7-cycle ultrasound-assisted ice recrystallization (US+IR) protocol of rice starch was performed followed by additional modification with amyloglucosidase (AMG) or maltogenic α-amylase (MA). To discriminate effects of the incubation conditions on the starch, control samples were prepared under the same conditions in the absence of enzyme.

3.1. Granular morphology, specific surface area and total pore volume

SEM micrographs demonstrate that the native rice starch exhibited a polyhedral morphology and a relatively smooth surface with few pits (Fig. 1, NR). The US+IR treatment did not have significant destructive effects on the general granular shape (Fig. 1, A1 and B1). However, this treatment induced granule roughness, additional grooves and shallow indentations at the surface. The specific indentation surface effect is possibly caused by a series of complex events including in granule, ice recrystallization exerting local high pressure in ordered crystalline structures at the surface, resulting in the granular surface indentations [5,7]. Additionally, surface roughness is possibly induced by cavitation force of ultrasonic during thawing process, an effect caused by collage of microbubbles, resulting in a jet of water directed onto the granule surface [31–33].

The combined effects of US+IR and enzymatic hydrolysis were visible in the granular morphology as holes and fissures (Fig. 1, A2 and B2). MA was demonstrated more active on the starch granules than AMG, resulting in perforated granules seemingly deeper than for the AMG treatment. This discrepancy could be due to the hydrolytic mechanism of MA exhibiting both *endo*- and *exo*-activity [21,34] as compared to AMG having only exo-activity.

The specific surface area and total pore volume of starch samples were calculated based on nitrogen adsorption isotherms using the BET method. Surprisingly, the US+IR treatment had no effect on the specific surface area (S_{BET}) and total pore volume relative to native rice starch (Fig. 2). However, the combination US+IR and enzymatic hydrolysis resulted in an increase in S_{BET} and total pore volume. The highest S_{BET} and total pore volume were found for the US+IR→MA sample (1.96 $m^2\ g^{-1}$ and $7.26 \times 10^{-3}\ cm^3\ g^{-1}$, respectively). These data were in accordance with SEM (Fig. 1, B2) clearly visualizing more pores at the granule surface of the US+IR → MA sample.

Table 1
Relative crystallinity, amylose content, swelling capacity, solubility index and rate coefficient (k) for digestion of modified starch.

Samples	Relative crystallinity (%)	Amylose content (%)	Swelling capacity (g/g)	Solubility index (%)	k (min^{-1}) x10^{-3}
Native	23.8 ± 1.0 c	29.5 ± 0.5 c	2.8 ± 0.1 d	0.47 ± 0.19 a	2.07 ± 0.31 a
US+IR → no AMG	20.6 ± 0.2 a	28.1 ± 0.2 b	2.7 ± 0.1 c	0.94 ± 0.21 b	2.97 ± 0.06 c
US+IR → AMG	21.8 ± 0.2 ab	26.5 ± 0.1 a	2.6 ± 0.0 b	0.98 ± 0.28 b	2.50 ± 0.26 b
US+IR → no MA	20.7 ± 0.0 a	27.9 ± 0.3 b	2.7 ± 0.1 c	0.98 ± 0.26 b	2.60 ± 0.10 bc
US+IR → MA	22.3 ± 0.1 b	26.6 ± 0.1 a	2.1 ± 0.1 a	1.37 ± 0.25 c	2.30 ± 0.17 ab

Values followed by different letters within a column are significantly different ($p < 0.05$).

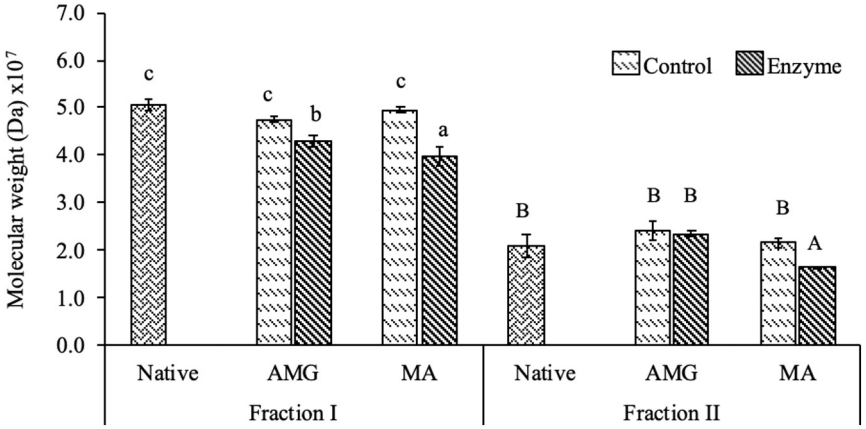

Fig. 3. Molecular weight of the amylopectin (Fraction I) and amylose (Fraction II) of native and US+IR treated starch with (enzyme, AMG and MA) and without (control) enzymatic hydrolysis. The lower-case letters express the significant difference (0.05) for fraction I and the upper-case letters for fraction II.

3.2. Crystalline structure

The crystalline structure of rice starch processed with US+IR and combined with enzyme hydrolysis was measured by wide-angle X-ray scattering. All starch samples exhibited similar WAXS patterns which strong reflections at 15°, 17°, 18°, and 23° (2θ), typical for the A-type crystalline polymorph (data not shown). This data documents that the combined treatment did not significantly affect the remaining crystalline arrangement in the starch granules. However, the relative crystallinity, as calculated from the WAXS diffractograms, was significantly decreased after US+IR compared to native rice starch and slightly increased after the combination with enzyme compared to the corresponding control samples (Table 1). The crystallinity of native rice starch was 23.8% that fell to 20.6–20.7% after US+IR and increased to 21.8–22.3% following enzyme treatment. This result indicates a synergistic effect of ice crystal growth in the starch granule [7] and the shear force from the ultrasonic energy causing weakening of double helices and partly disruption crystalline starch granule sections [19,33]. The 5.8% and 7.6% increase in crystallinity for AMG or MA, respectively, was likely due to the combined effects of exposure of starch chains to the enzymes, rearranged by the ultrasonic treatment [19] and ice recrystallization events taking place mainly in amorphous region, as deduced for the increased crystallinity.

3.3. Apparent amylose

For native rice starch, the apparent amylose content was 29.5% (Table 1). The apparent amylose of US+IR treated starch samples decreased by approximately 1.5% units. It was noteworthy that the decrease in amylose content can be induced not only by ice crystal growth, which possibly induces exudation of amylose from the amorphous part of the granules [35,36] but also by molecular degradation during US+IR repeated cycles since amylose, mostly located in amorphous part, would be susceptible for ultrasonic degradation. Following the combined hydrolase treatment, the apparent amylose was further decreased to 21.8 and 22.3% for AMG and MA, an enzyme-related decrease by 1.2 and 1.6% units, respectively. These data suggest that the US+IR treatment has exposed new amorphous granule surfaces allowing increased accessibility of enzymes into starch granules causing more enzymatic efficient hydrolysis of amylose. This result was consistent with the crystallinity data that the combined treatment with enzyme had higher crystallinity than their specific control.

3.4. Starch molecular weight distribution

Molecular weight distributions of the starch fractions were obtained using size-exclusion chromatography with triple detection array (SEC-TDA). The chromatogram showed a typical bimodal distribution mainly originating from high molecular mass amylopectin and lower molecular mass amylose (Supplementary Fig. 1) with fraction I and fraction II that refer to high (mainly amylopectin) and low (mainly amylose) molecular weight, respectively. No significant changes were found for the US+IR treatments (Fig. 3) demonstrating that no significant breakdown of the starch was induced by this treatment. As expected, hydrolase treatment caused some significant decreases in the molecular weights, but mainly for fraction I (Fig. 3). Only the MA treatment further decreased the molecular weight of fraction II. This may be explained by different mechanism of the AMG and MA, MA having both *endo*- and *exo*-activity [37]. These data are in compliance with the morphological granule (Fig. 1) data showing more extensive effect for the MA.

3.5. Swelling capacity and solubility

The swelling capacity of was substantially reduced by the US+IR treatment and enzyme treatment further reduced this parameter (Table 1). The most dramatic decrease in swelling capacity was observed for the US+IR → MA treated sample, which was the most affected sample with respect to morphology and reduction in molecular size. The data suggest that the nature of the modifications are attributed to the internal rearrangement of starch chains in a manner to restrict water absorption and granular swelling [38]. The more extensive

Table 2
Pasting properties of starch samples.

Samples	Pasting temp (°C)	Peak viscosity (cP)	Breakdown (cP)	Final viscosity (cP)	Setback (cP)
Native	79.4 a	930 b	100 a	961 b	134 ab
US+IR → no AMG	82.8 b	1150 d	185 c	1100 e	136 ab
US+IR → AMG	88.7 c	1050 c	175 c	1000 c	126 ab
US+IR → no MA	83.6 b	1030 c	149 b	1080 d	146 b
US+IR → MA	93.7 d	770 a	111 a	769 a	110 a

Values followed by different letters within a column are significantly different ($p < 0.05$).

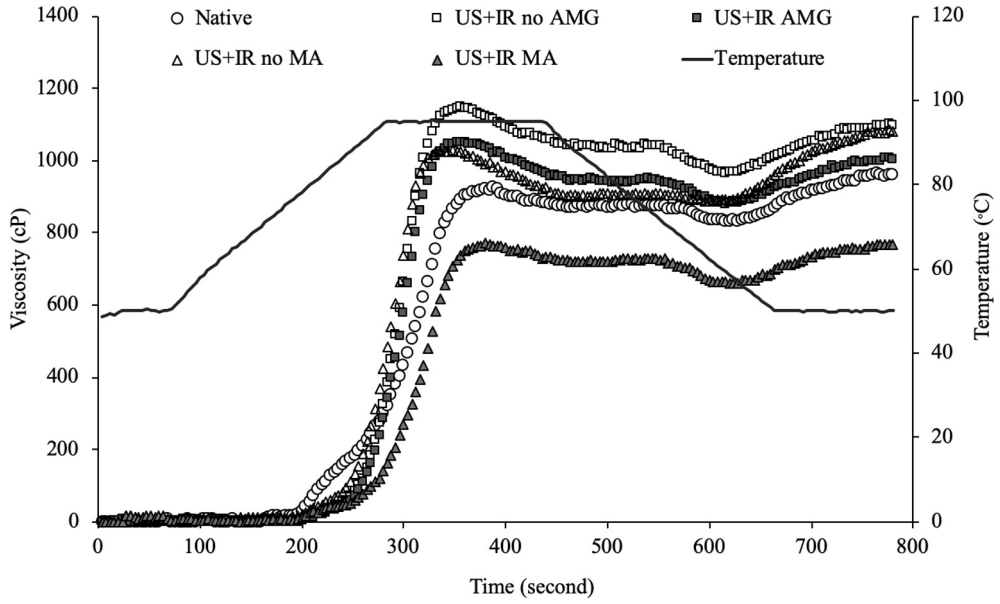

Fig. 4. RVA profiles of native, US+IR treated starch with enzyme (AMG and MA) and without (buffer control) enzyme.

porous and/or fissure structure of this sample also suggest collapse of inner structures following enzymatic modification (as seen in Fig. 1, A2 and B2) resulting in reduced capacity for water absorption.

The solubility showed an opposite trend as compared to the swelling capacity, i.e. enhanced solubility following modifications (Table 1). For US+IR treatment, increased solubility could be due to a synergistic effect of physical stress induced by ice formation and shear force created by ultrasonic cavitation to induce exudation of small starch fragments. The most prominent increase in solubility was found by US+IR→MA, again explained by *endo*- and *exo*-activities of MA producing small molecular and soluble starch fragments.

3.6. Pasting properties

Pasting properties are related to the gel viscosity, the stability of starch paste and retrogradation tendency. Both the US+IR and the following enzyme treatments markedly increased the peak temperature from 79.4 up to 93.7 °C (Table 2 and Fig. 4). These data agree with the swelling capacity data (Table 1) showing suppressed swelling following modification. The US+IR treated sample exhibited an increased peak viscosity, breakdown and final viscosity while setback values were not significantly different. However, following enzyme hydrolysis, those pasting parameters were prominently decrease. The US+IR → MA sample fell down to, or below, that of the native starch sample.

The increase of peak viscosity is supposedly attributed to the weakening of starch interior interactions by US+IR reducing granule integrity, facilitating penetrate of water into the starch granules. However, since the US+IR treatment also caused the amylose leaching (as discussed in Section 3.3) decreased amylose content can provide the same effects [39,40]. The enzyme treatments significantly decreased the peak viscosity compared to their corresponding US+IR samples. This reduction is supposedly attributed to the hydrolytic reactions resulting in partly disintegrated the starch granules (Fig. 1) and decreased molecular weights of the starch fractions (Fig. 3).

The breakdown parameter is related to the thermal stability of the swollen starch granules in the starch paste during heating and shearing, i.e. higher breakdown indicates less resistance to shear force [41,42]. The increased breakdown value of US+IR treated starch, might be due to the weakening or complete rupture of intra- and inter-molecular hydrogen bonds of starch molecules. This view is supported by our WAXS data (Table 1) showing reduction of crystallinity after US+IR treatment. However, the breakdown values were decreased following hydrolytic treatment, an effect possibly shortening and solubilization of starch chains causing loss compact granules. Alternatively, the reduction of breakdown value might be because of the peak viscosity decreasing after enzymatic treatment. Final viscosity and setback value are represented to the re-association during cooling of the main amylose that released following. Despite the decreased amylose the US+IR treatments resulted in increased final viscosities which we suggest is an effect release of linear starch fragments by the US+IR treatments prone to re-associate following cooling of the starch paste. Enzyme treatment expectedly decreased both the final viscosity and setback parameters as expected from the hydrolytic activity. The MA treatment displayed the most substantial effect due to its *endo*-activity, severely reducing the molecular size.

3.7. Thermal properties

The thermal properties data, as determined by DSC, were evaluated from the parameters including Ti, identified as a minor increase in gelatinization preceding the major gelatinization point, To: onset temperature, Tp: peak temperature, Tc: conclusion temperature, ΔT = Tc-Ti and ΔH: gelatinization enthalpy (Table 3 and Fig. 5). The Ti of the US+IR treated starch was significantly higher than the native starch and this parameter further increased after enzyme treatment. The increase of Ti could be an effect of molecular annealing taking place during US+IR treatment. The annealing effect is described as a more ordered structure of the arrangement of double helices that can result in increased granular stability [43]. This result is in agreement with the previous observations showing increased pasting temperature (Table 2 and Fig. 4) and reduced swelling capacity (Table 1) for the US+IR samples.

Table 3
Thermal properties of starch samples.

Samples	Ti (°C)	To (°C)	Tp (°C)	Tc (°C)	Tc-Ti (°C)	ΔH (J/g °C)
Native	60.8 a	70.3 ab	75.5 d	80.2 c	19.4 e	10.1 b
US+IR → no AMG	65.4 b	70.1 a	74.5 a	78.4 a	13.0 c	8.9 a
US+IR → AMG	66.4 c	70.3 ab	74.5 a	78.3 a	11.9 a	9.1 a
US+IR → no MA	65.4 b	70.6 b	74.9 b	78.9 b	13.5 d	9.3 a
US+IR → MA	66.5 c	71.2 c	75.1 c	79.2 b	12.6 b	10.2 b

Ti = initial temperature, To = onset temperature, Tp = peak temperature, Tc = conclusion temperature, Tc-Ti = gelatinization temperature range and ΔH = gelatinization enthalpy.
Different small caused letters within a column denote significant differences ($p < 0.05$).

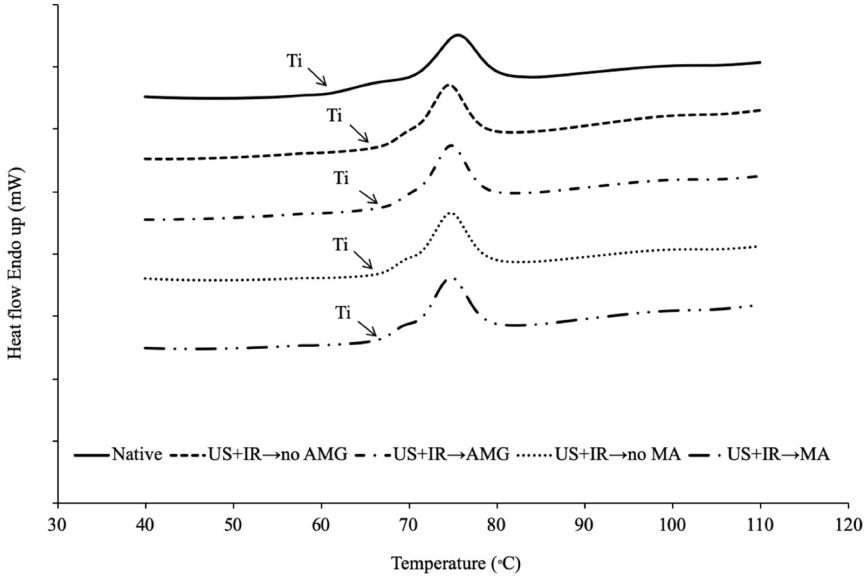

Fig. 5. DSC thermograms of native and starch treated samples. Ti = initial temperature. One tick mark of y axis = 1 mW.

Additionally, the of US+IR treated starches showed slightly decreased Tp, Tc and ΔH values while To were insignificantly different from native starch. The decrease could be attributed to disruption of crystalline part of starch granules [7] as shown by our crystallinity data (Table 1). Interestingly, the US+IR→MA significantly increased To, Tp, Tc and ΔH compared to buffer control. The higher dissolution transition temperature and ΔH are likely due to the increased perfection of double helices of starch granules caused by the hydrolysis of MA occurred in amorphous part. This result is also consistent with the crystallinity data which distinctly increased after the combination with MA. Higher degree of crystallinity has been implied to stabilize starch granules [44]. Therefore, the US+IR combined with enzymes, especially MA, are more resistant to thermally processing.

3.8. Rate of digestion

To investigate the susceptibility of the modified starch samples, the rate of digestion by PPA (porcine pancreatic amylase) and AMG was carried out. The digestion rate constants (k-values) of US+IR treated starch was markedly higher than of native starch (Table 1) demonstrating higher susceptibility to digestive PPA and AMG catalyzed degradation. This increased hydrolytic susceptibility of the US+IR treated starches could be attributed to the combined ice crystallization and ultrasonic-mediated destruction of the crystalline structure, increasing more vulnerable amorphous regions more readily accessed by the dietary hydrolytic enzymes. These data are in accordance with the WAXS data showing decreased crystallinity by US+IR treatment. However, as expected from the action of the hydrolases during preparation of the modified starches, the combined treatments with hydrolases exhibited lower k-value than those of control, i.e. increase enzyme resistance. These results are therefore an effect of the removal of susceptible starch segments and related to the increased crystalline rigidity of the products, having increased crystallinity and melting enthalpy following enzyme treatment.

4. Conclusions

Significant differences in the morphological, structural, physicochemical and digestible characteristics of rice starch modified by 7 repeated cycles of US and IR as well as subsequent enzyme-assisted hydrolysis were investigated. The US+IR treatment produced granules with more grooves and shallow indentations. Combined with AMG or MA treatments, created pores and fissures on the granular surface resulting in increased specific surface area. The US+IR treatment decreased the amylose content, relative crystallinity, swelling capacity and the enthalpy of dissolution. Subsequent AMG or MA treatments further decreased amylose content, swelling capacity, molecular weight, peak viscosity, breakdown, final viscosity, setback value and the rate coefficient of amylolytic degradation. Specifically, the US+IR→MA treatment resulted in high crystallinity and enthalpy as compared to AMG making theses treated-starch more thermostable for processing. Overall, the combination of US+IR and enzyme catalysis provides an efficient and new method for producing porous rice starch that can be used in various food applications as carrier agents for volatile compounds, protecting the sensitive substances and for further chemical modifications.

Supplementary data to this article can be found online at https://doi.org/10.1016/j.ijbiomac.2019.12.144.

CRediT authorship contribution statement

Thewika Keeratiburana: Methodology, Formal analysis, Investigation, Writing - original draft. **Aleksander Riise Hansen:** Investigation. **Siriwat Soontaranon:** Software. **Sunanta Tongta:** Conceptualization, Data curation, Writing - review & editing. **Andreas Blennow:** Conceptualization, Data curation, Writing - review & editing.

Acknowledgements

This research was supported by the Royal Thai Government Scholarship (Ministry of Higher Education, Science, Research and Innovation), Thailand and partly supported by Archer Daniels Midland (ADM) Company, Decatur IL, USA. The SEC was provided by grant from the Carlsberg Foundation. Novozymes A/S is appreciatively acknowledged for providing MA. The authors would like to thank Dr. Eric Bertoft for fruitful discussions.

References

[1] L. Amagliani, J. O'Regan, A.L. Kelly, J.A. O'Mahony, Chemistry, structure, functionality and applications of rice starch, J. Cereal Sci. 70 (2016) 291–300.
[2] Y. Benavent-Gil, C.M. Rosell, Morphological and physicochemical characterization of porous starches obtained from different botanical sources and amylolytic enzymes, Int. J. Biol. Macromol. 103 (2017) 587–595.

[3] B. Zhang, D. Cui, M. Liu, H. Gong, Y. Huang, F. Han, Corn porous starch: preparation, characterization and adsorption property, Int. J. Biol. Macromol. 50 (2012) 250–256.
[4] H. Tao, P. Wang, B. Ali, F. Wu, Z. Jin, X. Xu, Structural and functional properties of wheat starch affected by multiple freezing/thawing cycles, Starch/Stärke 67 (2015) 683–691.
[5] H. Tao, J. Yan, J. Zhao, Y. Tian, Z. Jin, X. Xu, Effect of multiple freezing/thawing cycles on the structural and functional properties of waxy rice starch, PLoS One 10 (2015).
[6] S. Yu, Y. Zhang, H. Li, Y. Wang, C. Gong, X. Liu, X. Zheng, N.K. Kopparapu, Effect of freeze-thawing treatment on the microstructure and thermal properties of non-waxy corn starch granule, Starch/Stärke 67 (2015) 989–1001.
[7] A.Q. Zhao, L. Yu, M. Yang, C.J. Wang, M.M. Wang, X. Bai, Effects of the combination of freeze-thawing and enzymatic hydrolysis on the microstructure and physicochemical properties of porous corn starch, Food Hydrocoll. 83 (2018) 465–472.
[8] S. Charoenrein, N. Preechathammawong, Effect of waxy rice flour and cassava starch on freeze-thaw stability of rice starch gels, Carbohydr. Polym. 90 (2012) 1032–1037.
[9] M. Sujka, J. Jamroz, Ultrasound-treated starch: SEM and TEM imaging, and functional behaviour, Food Hydrocoll. 31 (2013) 413–419.
[10] F. Zhu, Impact of ultrasound on structure, physicochemical properties, modifications, and applications of starch, Trends Food Sci. Technol. 43 (2015) 1–17.
[11] Q.T. Le, C.K. Lee, Y.W. Kim, S.J. Lee, R. Zhang, S.G. Withers, Y.R. Kim, J.H. Auh, K.H. Park, Amylolytically-resistant tapioca starch modified by combined treatment of branching enzyme and maltogenic amylase, Carbohydr. Polym. 75 (2009) 9–14.
[12] E.J. Oh, S.J. Choi, S.J. Lee, C.H. Kim, T.W. Moon, Modification of granular corn starch with 4-α-glucanotransferase from Thermotoga maritima: effects on structural and physical properties, J. Food Sci. 73 (2008).
[13] C.K. Lee, Q.T. Le, Y.H. Kim, J.H. Shim, S.J. Lee, J.H. Park, K.P. Lee, S.H. Song, H.A. Joong, S.J. Lee, K.H. Park, Enzymatic synthesis and properties of highly branched rice starch amylose and amylopectin cluster, J. Agric. Food Chem. 56 (2008) 126–131.
[14] Y. Benavent-Gil, C.M. Rosell, Comparison of porous starches obtained from different enzyme types and levels, Carbohydr. Polym. 157 (2017) 533–540.
[15] A. Dura, W. Błaszczak, C.M. Rosell, Functionality of porous starch obtained by amylase or amyloglucosidase treatments, Carbohydr. Polym. 101 (2014) 837–845.
[16] A. Dura, C.M. Rosell, Physico-chemical properties of corn starch modified with cyclodextrin glycosyltransferase, Int. J. Biol. Macromol. 87 (2016) 466–472.
[17] N.S. Yussof, U. Utra, A.K. Alias, Hydrolysis of native and cross-linked corn, tapioca, and sweet potato starches at sub-gelatinization temperature using a mixture of amylolytic enzymes, Starch/Stärke 65 (2013) 285–295.
[18] D. Wang, X. Ma, L. Yan, T. Chantapakul, W. Wang, T. Ding, X. Ye, D. Liu, Ultrasound assisted enzymatic hydrolysis of starch catalyzed by glucoamylase: investigation on starch properties and degradation kinetics, Carbohydr. Polym. 175 (2017) 47–54.
[19] M. Li, J. Li, C. Zhu, Effect of ultrasound pretreatment on enzymolysis and physicochemical properties of corn starch, Int. J. Biol. Macromol. 111 (2018) 848–856.
[20] Y. Wu, X. Du, H. Ge, Z. Lv, Preparation of microporous starch by glucoamylase and ultrasound, Starch/Stärke 63 (2011) 217–225.
[21] C. Christophersen, D.E. Otzen, B.E. Norman, S. Christensen, T. Schäfer, Enzymatic characterisation of novamyl®, a thermostable α-amylase, Starch/Stärke 50 (1998) 39–45.
[22] H.J. Cha, H.G. Yoon, Y.W. Kim, H.S. Lee, J.W. Kim, K.S. Kweon, B.H. Oh, K.H. Park, Molecular and enzymatic characterization of a maltogenic amylase that hydrolyzes and transglycosylates acarbose, Eur. J. Biochem. 253 (1998) 251–262.
[23] H.S. Lee, J.H. Auh, H.G. Yoon, M.J. Kim, J.H. Park, S.S. Hong, M.H. Kang, T.J. Kim, T.W. Moon, J.W. Kim, K.H. Park, Cooperative action of α-glucanotransferase and maltogenic amylase for an improved process of isomaltooligosaccharide (IMO) production, J. Agric. Food Chem. 50 (2002) 2812–2817.
[24] S. Brunauer, P.H. Emmett, E. Teller, Adsorption of gases in multimolecular layers, J. Am. Chem. Soc. 60 (1938) 309–319.
[25] S. Boonna, S. Tongta, Structural transformation of crystallized debranched cassava starch during dual hydrothermal treatment in relation to enzyme digestibility, Carbohydr. Polym. 191 (2018) 1–7.
[26] H.A.M. Wickramasinghe, A. Blennow, T. Noda, Physico-chemical and degradative properties of in-planta re-structured potato starch, Carbohydr. Polym. 77 (2009) 118–124.
[27] J.D. Klucinec, D.B. Thompson, Fractionation of high-amylose maize starches by differential alcohol precipitation and chromatography of the fractions, Cereal Chem. 75 (1998) 887–896.
[28] W. Sorndech, S. Meier, A.M. Jansson, D. Sagnelli, O. Hindsgaul, S. Tongta, A. Blennow, Synergistic amylomaltase and branching enzyme catalysis to suppress cassava starch digestibility, Carbohydr. Polym. 132 (2015) 409–418.
[29] C.M. Rosell, W. Yokoyama, C. Shoemaker, Rheology of different hydrocolloids-rice starch blends. Effect of successive heating-cooling cycles, Carbohydr. Polym. 84 (2011) 373–382.
[30] H.N. Englyst, S.M. Kingman, J.H. Cummings, Classification and measurement of nutritionally important starch fractions, Eur. J. Clin. Nutr. 46 (Suppl. 2) (1992) S33–S50.
[31] M. Sujka, Ultrasonic modification of starch – impact on granules porosity, Ultrason. Sonochem. 37 (2017) 424–429.
[32] Y.Y.J. Zuo, P. Hébraud, Y. Hemar, M. Ashokkumar, Quantification of high-power ultrasound induced damage on potato starch granules using light microscopy, Ultrason. Sonochem. 19 (2012) 421–426.
[33] J. Zhu, L. Li, L. Chen, X. Li, Study on supramolecular structural changes of ultrasonic treated potato starch granules, Food Hydrocoll. 29 (2012) 116–122.
[34] H. Goesaert, L. Slade, H. Levine, J.A. Delcour, Amylases and bread firming - an integrated view, J. Cereal Sci. 50 (2009) 345–352.
[35] J. Szymońska, K. Wodnicka, Effect of multiple freezing and thawing on the surface and functional properties of granular potato starch, Food Hydrocoll. 19 (2005) 753–760.
[36] C. Zhang, J.A. Han, S.T. Lim, Characteristics of some physically modified starches using mild heating and freeze-thawing, Food Hydrocoll. 77 (2018) 894–901.
[37] M. Miao, S. Xiong, F. Ye, B. Jiang, S.W. Cui, T. Zhang, Development of maize starch with a slow digestion property using maltogenic α-amylase, Carbohydr. Polym. 103 (2014) 164–169.
[38] Y. Ding, F. Luo, Q. Lin, Insights into the relations between the molecular structures and digestion properties of retrograded starch after ultrasonic treatment, Food Chem. 294 (2019) 248–259.
[39] J. Jane, Y.Y. Chen, L.F. Lee, A.E. McPherson, K.S. Wong, M. Radosavljevic, T. Kasemsuwan, Effects of amylopectin branch chain length and amylose content on the gelatinization and pasting properties of starch, Cereal Chem. 76 (1999) 629–637.
[40] R. Juhász, A. Salgó, Pasting behavior of amylose, amylopectin and their mixtures as determined by RVA curves and first derivatives, Starch/Stärke 60 (2008) 70–78.
[41] F. Zhu, R. Mojel, G. Li, Physicochemical properties of black pepper (*Piper nigrum*) starch, Carbohydr. Polym. 181 (2018) 986–993.
[42] A.A. Karim, M.Z. Nadiha, F.K. Chen, Y.P. Phuah, Y.M. Chui, A. Fazilah, Pasting and retrogradation properties of alkali-treated sago (Metroxylon sagu) starch, Food Hydrocoll. 22 (2008) 1044–1053.
[43] L. Jayakody, R. Hoover, Effect of annealing on the molecular structure and physicochemical properties of starches from different botanical origins - a review, Carbohydr. Polym. 74 (2008) 691–703.
[44] A. Kaur, N. Singh, R. Ezekiel, N.S. Sodhi, Properties of starches separated from potatoes stored under different conditions, Food Chem. 114 (2009) 1396–1404.